RESEARCH ARTICLE

# Soil Erosion Estimation Using Remote Sensing Techniques in the Shirvan Plain of the Republic of Azerbaijan

S. Kh. Shkurov

*Doctor of Philosophy of Agrarian Sciences, Institute of Soil Science and Agrochemistry of ANAS, Baku-2020, Azerbaijan*

## ABSTRACT

Soil erosion is one of the major environmental problems in terms of soil degradation in the Shirvan plain of the Republic of Azerbaijan. Soil erosion leads to significant on- and off-site impacts such as significant decrease in the productive capacity of the land and sedimentation. The key aspects influencing the quantity of soil erosion mainly rely on the vegetation cover, topography, soil type, and climate. This research studies the quantification of soil erosion under different levels of data availability in the Shirvan plain. Remote sensing (RS) and Geographic Information System (GIS) techniques have been implemented for the assessment of the data, applying the Revised Universal Soil Loss Equation (RUSLE) for the calculation of the risk of erosion. Thirty soil samples were randomly selected for the calculation of the erodibility factor, based on calculating the $K$-factor values derived from soil property surfaces after interpolating soil sampling points. Soil erosion risk map was reclassified into five erosion risk classes and 25.3% of the Shirvan plain is under severe risk (190,740 ha). GIS and RS proved to be powerful instruments for mapping soil erosion risk, providing sufficient tools for the analytical part of this research. The mapping results certified the role of RUSLE as a decision support tool.

**Key words:** Ecosystem, erosion, slopes, cross country, topography, soil type, climate, land productivity, sediment, remote sensing, soil degradation, etc.

## INTRODUCTION

Evaluating soil erosion risks are a difficult under taking task due to several concurrent processes, which affect individually other multifaceted interactions and continue at amounts that vary in both time and space.[2] Soil erosion is caused by the erosive forces of wind or water. In this publication, we focus our attention on concepts surrounding water-induced soil erosion. This type of erosion threatens our ability as humans to sustain our global population with food and fiber and is closely linked to economic vitality, environmental quality, and human health concerns. Roughly 75 billion tons of fertile topsoil is lost worldwide from agricultural systems every year.

Erosion in the Republic of Azerbaijan, the total area of affected lands was 3144.7 thousand hectares, which is 36.4% of the country territory. About 38.8% (1220.1 ha) of eroded lands of the republic are weak, 29.4% (924 ha) are medium, and 31.8% (1000.6 ha) were severely eroded. According to researchers, in the watershed and transit areas of river basins located in mountainous areas, 70–80% of the soil cover is eroded under complex geomorphological conditions.[1]

Soil erosion occurs when parts of the soil are shifted around due to rainfall, wind, and ice melt. This is a natural process, but human activity can speed it up. The best way to combat soil erosion? Preventing it in the first place. Luckily, there are some additional

**Address for correspondence:**
S. Kh. Shkurov
E-mail:volqa_5@mail.ru

methods that can also help you reverse the impacts of soil attrition.[8]

With the presence of Geographic Information Systems (GIS) competencies, the efforts have been directed to be based on spatially distributed models simulating erosion dynamics and surface runoff of more complex and larger catchments.[14,10] Several models have been developed and used for either research or operational purposes. Some of the most known soil erosion models are USLE (Universal Soil Loss Equation, 1965), EPIC (Erosion/Productivity Impact Calculator, 1984), EUROSEM (European Soil Erosion Model, 1993), RUSLE (Revised USLE, 1997), Rill Grow (a model for rill initiation and development, 1998), SEMMED (Soil Erosion Model for Mediterranean Regions, 1999), EGEM (Ephemeral Gully Erosion Model, 1999), PESERA (Pan-European Soil Erosion Risk Assessment, 2003), and so forth. Soil erosion models can be distinguished as mechanistic (or process based) when they simulate the physical erosion processes by specific formulas or empirical when they calculate erosion based on regression of soil loss based on the physical properties of land and climate features.[11,12] They also can be characterized as dynamic when the time is a contained parameter. Long-term models are based on accumulated temporal data while event-based models describe single events.[10,13]

The soil erosion estimation models are focused on the identification and quantification of the erosion processes and the controlling factors, resulting in the sequential erosion models development beginning with the universal erosion equation (USLE) realized by Wischmeier and Smith,[15] followed by a modified equation (MUSLE) for the quantification of the alluvium resulting from erosion following each rainfall realized by Williams,[16] and eventually computerized and more complex equation (RUSLE) developed by Renard et al.[17]

The most important climatic variable in soil erosion processes is rainfall erosivity, which is related to rainfall amount and rainfall intensity.[18,19] Plants vegetative cover in addition to crop residues reduce soil erosion potential, due to the fact that the vegetation cover protects and leads to slowing down surface runoff movement and enhancing surplus surface water infiltration.[20,21] Type, extent, and quantity of the vegetation cover are the limiting factors of soil erosion effectiveness.[22,23]

The main aim of this research is to quantify the soil erosion in the Shirvan plain, which is the main agricultural zone in the Republic of Azerbaijan through examining the soil erodibility K-factor under different levels of soil data availability using the RUSLE model.

## MATERIALS AND METHODS

Shirvan steppe is part of the Kur-Araz Lowland of Azerbaijan and is located on the left bank of the Kura river, in the area between the Kura river and the Caspian sea. It is one of the areas where flat mud volcanoes are spread. It has Chala lakes fed by the Upper Shirvan canal. The elevation of the steppe ranges between 16 m and 100 m. The steppe has gray desert soil. Its vegetation is halophytic and wormwood, with estuary meadows. The upper Shirvan water channel was directed from the Mingachevir reservoir to irrigate the land. X = 165672.168, Y = 4523537.932 and X = 327493.967, Y = 4423734.657 located between the coordinates. Summer is very hot and dry. On some days, the temperature reaches 36–40°C. The second is the temperate hot semi-desert and dry steppe climate with dry winters. The annual number of sunny hours in the area varies between 2100 and 2400. The average annual temperature in the area varies between 14 and 150.

In the Shirvan plain, soil temperature is unevenly distributed depending on air temperature, soil history, and vegetation cover. The lowest average monthly temperature is 1–3.50 and the highest is 30–35°C on the soil surface of the plain. Precipitation is unevenly distributed in the Shirvan plain. The amount of precipitation in the area varies from 250 to 510 mm. Most precipitation falls in spring and autumn. It snows very little. The thickness of snow cover is 20–25 cm, the settling time is 10–13 days. Winds blowing in the Shirvan plain are formed under the influence of local conditions and incoming air masses. These winds often change direction due to the change of seasons.[3]

The rivers entering the Shirvan plain are of transit nature. These rivers belong to the Kura basin and start from the altitude of 2000 to 3500 m on the southern slope of the main Caucasus range. Alijanchay, Turyanchay, Goychay, and Girdimanchay are divided into a number of branches after rising from the lowlands to the Shirvan plain.

Garasu rivers are formed from the water that flows underground from the surface of the supply cones and

rises to the surface in the form of boils in the outer parts. The Turyanchay River begins at the foot of the Bazarduzu and Tufan peaks of the Main Caucasus Range, at an absolute height of 3680 m, and flows into the Kura at a height of 3.5 m, west of the city of Zardab. In the upper reaches, the catchment area of the Turyanchay is 1842 km², water consumption is 15.6 m³/s, and the annual flow is 491,000 m³. The Goychay river began at an altitude of 2500–3000 m at the foot of the Savalan Pass and Babadag Peak and flowed into the Garasu at an absolute height of 9 m. In connection with the subsequent reclamation measures, it was connected directly to the globe. The catchment area is 1770 km², the average annual water consumption is 12.5 m³/s. The length of the river is 50–60 km. Girdimanchay flowed into Garasu at an altitude of 9 m, starting from 3000 m at the foot of Babadag Peak. Later, it was discharged into the Kura River through an artificial bed. The catchment area is 232 km², water consumption is 2.34 km³/s. The length of the Shirvan plain is about 25.2 km. The density of the general river network of the Shirvan plain is 0.46–0.5 ka/km². The flow in the rivers of the Shirvan plain is uneven throughout the year. In addition to the rivers with a constant flow mentioned above, there are many dry valleys and ravines of different lengths, starting from the low mountains and having a temporary flow during heavy rains. The largest lake in the Shirvan plain is Hajigabul.[3] Water is discharged from the Kura River to keep the water level stable in the lake, which has an area of about 16 km². The lake is currently drying up. The dry, arid climate of the Shirvan plain requires maximum use of irrigation. The Upper Shirvan canal, which starts from the Mingachevir reservoir and stretches for 123 km, allows to irrigate more than 47,000 hectares. The Shirvan plain rivers have rich groundwater resources. The food source of groundwater is rainwater, river water, and irrigation leaks. The groundwater level in the 5–6 km wide strip along the Kura river is 1 m deep, and in the Goychay ground cone, it is 1.5–2 m. The flow of groundwater in the Shirvan plain was very weak, mainly due to the general inclination of the plain. Mud volcanoes in the lowlands are also relatively affected by the mineralization of groundwater in the eastern part of the Shirvan plain.[2]

Soil erosion from irrigated fields has been discussed previously;[7,8] this article focuses on unique aspects of irrigation-induced soil erosion that is important when managing and simulating soil erosion on irrigated lands. Soil erosion mechanics can be divided into three components: Detachment, transport, and deposition. Water droplets and flowing water detach soil particles; flowing water then transports these detached particles downstream; deposition occurs when flowing water can no longer transport the soil particles because flow rate decreases as water infiltrates or as rill slope or roughness changes. Some particles are deposited within a few meters although others are transported off the field with runoff water. These mechanisms are the same for surface irrigation, sprinkler irrigation, and rainfall; however, there are some systematic differences between irrigation and rainfall erosion and especially between surface irrigation and rainfall.

Erosion rates as high as 145 Mg/ha in 1 h[9] and 40 Mg/ha in 30 min[10] were reported in some early surface irrigation erosion studies. These extreme losses do not represent a sustained seasonal rate. Within field erosion rates on the upper quarter of a furrow irrigated field can be 10–30 times more than the field average erosion rate.[12] Some soil eroded from the upper end of a field is deposited on the lower end, whereas some soil leaves the field with runoff. Losing topsoil from the upper end of the field can decrease crop yields by 25% when compared with the lower end of the field.[13] Sediment cannot be transported without runoff. Runoff is planned with many surface irrigation schemes to irrigate all areas of the field adequately.[25]

## Methodological framework

The methodology is implemented through several steps which led to the intermediate and the final results.[4-6] Initially, the $C$, $R$, $P$, and LS factors were calculated to be included in the RUSLE formula. Then, the $K$-factor was estimated from the soil samples using the USDA nomograph.[23] Later, three interpolation methods (radial basis function [RBF], inverse distance weighted, and ordinary kriging) were checked for their accuracy and the $K$-factor layer (thematic map) was created using the most accurate method. By multiplying the RUSLE factors calculated earlier ($C*R*P*$ LS) with the $k$-layers (thematic map), soil erosion risk thematic map was created. Finally, the erosion risk map was reclassified into five classes of risk.

The mathematical expression of RUSLE is

$$A = R*K* LS *C*P \quad (1)$$

Where $A$ is the average annual erosion rate (t ha−1 yr−1);

$R$ is the rainfall erosivity (MJ mm ha−1 h−1 yr−1);

$K$ is the soil erodibility (t ha h ha−1 MJ−1 mm−1);

LS is slope length and slope steepness factor (dimensionless);

$C$ is the correction coefficient for the effect of vegetation (dimensionless); and $P$ is the correction coefficient for the effect of erosion control measurements (dimensionless).

Digital elevation model (DEM) data were used DEM is highly accurate DEM covering all the land on earth with 30 m spatial resolution. Landsat 8 Operational Land Imager scene was acquired in 2019. Landsat 8 consists of 9 multispectral bands of 30 m spatial resolution and two thermal bands of 100 m spatial resolution in addition to the panchromatic bands of 15 m spatial resolution. Two full width at half maximum bands of 654.6 $\mu$m as red band and 864.7 $\mu$m as infrared band were exercised to drive normalized difference vegetation index (NDVI).

**Generation of R, K-, LS, C, and P factors**

Rainfall erosivity factor (R), estimation of the rainfall erosivity factor ($R$), is highly based on annual rainfall (mm), and when the annual rainfall is high, erosivity ($R$) is also high. Rainfall erosivity factor ($R$) was estimated based on total kinetic energy ($E$) and maximum intensity in 30 min ($I$) in an average year's rain, Barfield *et al.*[25]

According to Wischmeier,[27] the best predictor of $R$ was

$$R = \frac{1}{n}\sum_{j-1}^{n}[\sum_{k-1}^{m}(E)(\dot{I}_{30})K \quad (2)$$

Where, E is the total storm kinetic energy,

$I_{30}$ is the maximum 30-min rainfall intensity,

$j$ is the counter for each year used to produce the average,

$k$ is the counter for the number of storms in a year,

$m$ is the number of storms $n$ each year, and $n$ is the number of years used to obtain the average

$R$ rain kinetic energy ($E$) could be predicted by

$$E = 916 + (331)\log 10 (I) \quad (3)$$

$K$-factor (soil erodibility) is the one that will be mainly examined.

Using the stratified random sampling method, thirty points, randomly selected and stratified in regard to the geologic formations, were sampled for their necessary topsoil properties. Then, $K$ values were calculated according to the RUSLE formula for these methods.[24] Finally, the $K$ values were interpolated to produce a surface of $K$ values for the total area. Not only is soil texture the principal component affecting $K$ but also soil permeability and soil organic content are essential.[26] Proposed an algebraic approximation taking into consideration five different soil features (soil organic content, soil permeability, soil texture, soil structure, and soil coarse fragments) as follows:

$$K = [\frac{(2,1*10^4 M1,14(12-OM)+ \; 3,25(S-2)+2,5(P-3))}{100}]*0,1317 \quad (4)$$

Where, $M$ is the textural factor with $M=(m_{silt}+m_{vfs})*(100-m_c)$;

$mc$ (%) is clay fraction content (<0.002 mm);

$m_{silt}$ (%) is silt fraction content (0.002–0.05 mm);

$m_{vfs}$ (%) is very fine sand fraction content (0.05–0.1 mm);

OM (%) is the organic matter content;

$s$ is the soil structure;

and $p$ is the permeability class.

The slope factor (LS) refers to the topographic and/or the relief factor. The slope length factor L computes the effect of slope length on erosion and the slope steepness factor S computes the effect of slope steepness on erosion.

The topography-related parameters were derived from the DEM.[27]

Based on Wischmeier and Smith,[15] LS values were estimated as follows:

$$LS = \left(\frac{l}{72,6}\right)m(64,41sin^2\beta + 4.56\sin\beta) \quad (5)$$

Where, $\ell$ is the cumulative slope length in feet;

is the downhill slope angle;

$m$, is a slope contingent variable,

**Table 1:** Erosion risk classes (ERC) following Wischmeier and Smith[11]

| Erosion class | ERC 1 | ERC 2 | ERC 3 | ERC 4 | ERC 5 |
|---|---|---|---|---|---|
| Lost/ha/yea | 0–5 | 5–10 | 10–20 | 20–40 | >40 |
| Classification | Very slight | Slight | Moderate | Severe | Very severe |

0.5 if the slope angle is >1.86°,
0.4, on slopes of 1.72°–2.86°,
0.3, on slopes of 0.57°–1.52°,
and 0.2, on slopes <0.51°.

The cover management factor (C) is dimensionless for each grid cell ranging from 0 to 1 under standard fallow conditions. As the surface cover is added to the soil, the *C* factor value approaches 0. In general, the *C* factor is calculated based on derivation of NDVI and then reclassification of NDVI to extract the *C* factor with higher positive values of NDVI. Red band and infrared band of Landsat 8 were exercised to estimate NDVI as follows:

$$\text{NDVI} = \frac{(IR - R)}{(IR + R)} \qquad (6)$$

Where, *IR* is the infrared band and *R* is the red band. The support practice factor (P) is defined as the ratio of soil loss with a specific support practice to the corresponding soil loss with up and down cultivation. The lower the *P* value is, the more effective the conservation practice is deemed to be in reducing soil erosion. Usually, in practice, expert opinion is used to qualitatively assess this factor.

**Integration of factors for erosion risk mapping**

The erosion risk maps were generated by integrating all pre-estimated factors according to the RUSLE to create erosion map using *K*-factor values derived from soil sampling with interpolation. This was done using map algebra following the RUSLE method, where all layers generated previously were multiplied under GIS environment.[15]

**RESULTS AND DISCUSSION**

To assess the soil erosion risks in the study area, several applications and analyses were implemented [Table 1]. Each generated factor was thus fully described and processed. Regression was found between the mean annual precipitation 2010 and
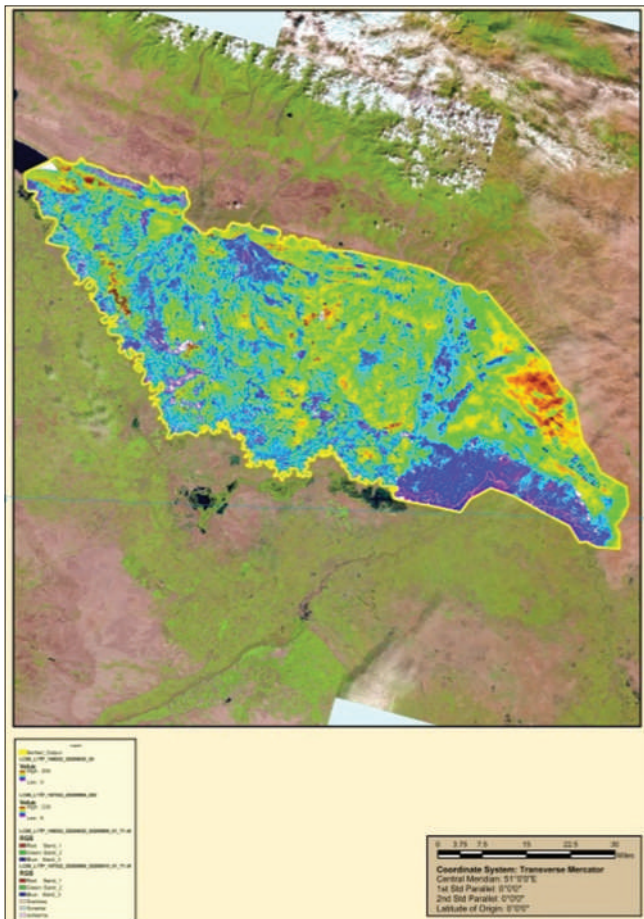


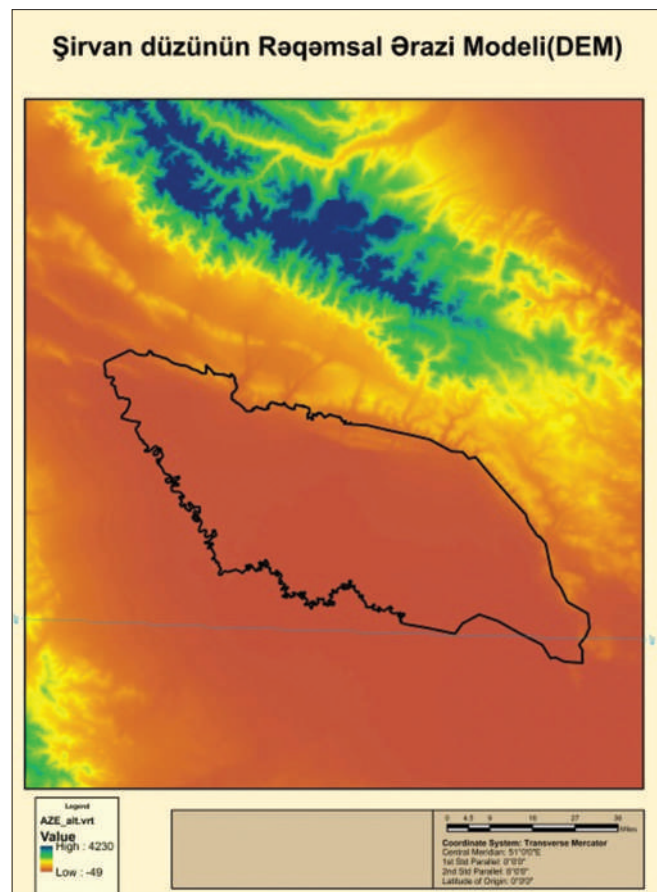**Figure 1:** Thematic map of rainfall erosivity factor (*R*) (MJ mm/ha year)



**Figure 2:** Thematic map of soil erodibility factor (*K*) (thahr/ha MJ mm)

2020 (mm/year) and the elevation to be read as
$$P = 1.53 * DEM + 20.8$$
The regression relationship was established before estimating the rainfall erosivity index as a function of average annual precipitation and elevation with $R^2$ of 0.667. The final thematic map for rainfall erosivity factor is shown in Figure 1. The standard error of estimate between the point and the surface



**Figure 3:** Thematic map of the length/slope (LS) factor

$K$-factor is 0.005 t ha h/ha MJ mm; $K$-factor is with an acceptable level of accuracy.[29]

Thematic map for the soil erodibility factor is shown in Figure 2. To determine LS factor adjusted by Moore and Burch[27-30] under GIS environment, the slope and flow length for each grid cell were estimated and illustrated in Figure 3. The effectiveness of the plant cover in reducing the raindrop impact depends on the height and the continuity of the canopy and the density of the ground cover. In this study, the $C$ factor was calculated using sigmoidal function derivation of NDVI to extract the $C$ factor.

The derivation of the NDVI values follows a monotonically decreasing sigmoid function with two control inflection points (0 and 1) which was used to define the fuzzy value of C factor in Figure 4. However, reclassification of the NDVI values was done to assign small values (near zero) for the $C$ factor for vegetated areas which are less risky in terms of erosion potential and big values (close to one) than sparsely vegetated areas and bare ground, which are more prone to erosion as it is shown in Figure 5.

Standard normal distribution function practiced on the NDVI values indicated that most of the values are around zero value, as demonstrated in Figure 6. Several negative values were reordered but there were more positive values indicating higher organic content.[31] The erosion risk map was generated by integrating all pre-estimated factors according to the RUSLE equation to create soil erosion map using $K$-factor values derived from
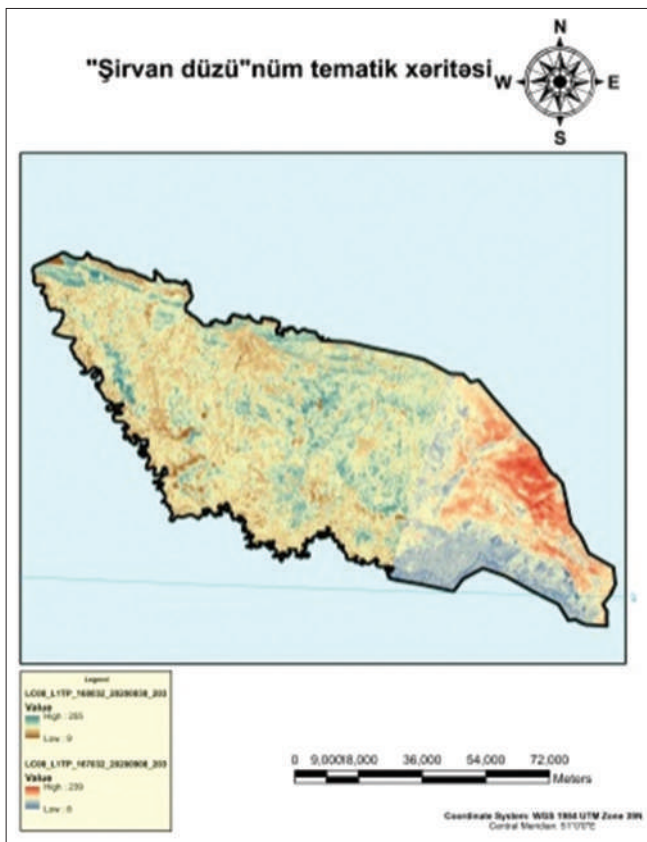


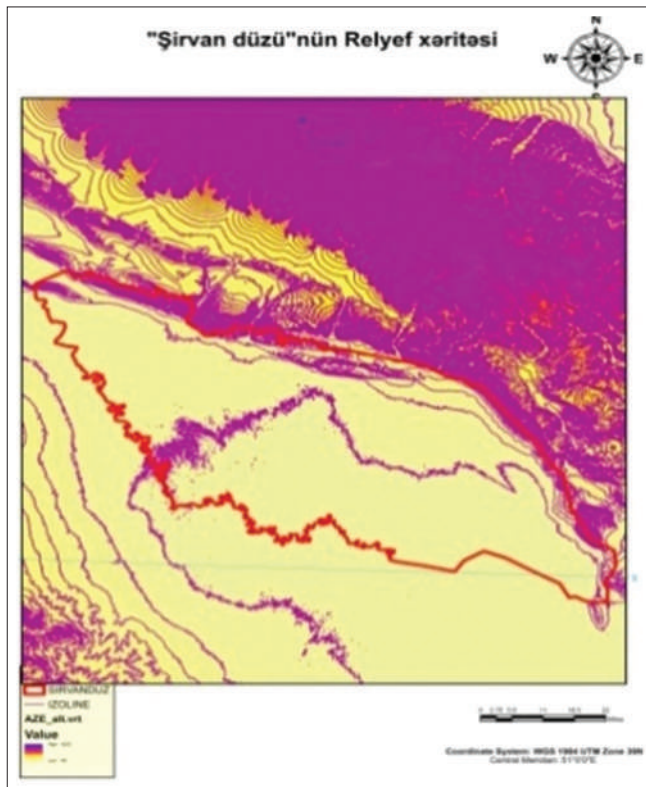**Figure 4:** Location of the study including sample sites

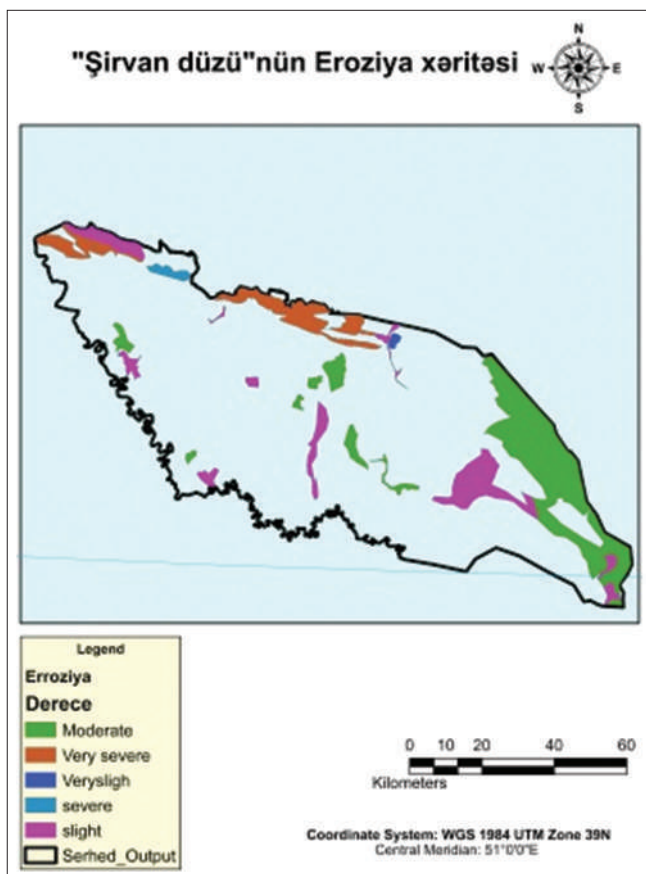**Figure 5:** Thematic map of the $C$ factor



**Figure 6:** Soil erosion classification map

soil sampling with interpolation of RBF with $R^2$ of 0.89.

Erosion is observed in the high hills of the Shirvan plain, along natural and artificial watersheds, in areas with dense drainage. In addition, the stream network carves its course and it carries the sediment that erodes as it flows.

This gives it more power to erode as there is more friction in the moving water, but it also deposits this material when it flows out of the upper stream onto the lower stream. Figure 6 demonstrates the proportion of each erosion risk class to the total basin area of Shirvan plain. Some of the total area is under slight risk (26.5%).

On the other hand, considerable areas are under severe risk (19.3%) and need further attention.

## CONCLUSION

Erosion risk values are ranked into classes, which is in accordance with RUSLE standards as it provides better identification of the area most prone to erosion. The dissimilarities discovered earlier seem to fade out.

GIS and remote sensing (RS) are inevitable technological environments when implementing RUSLE for assessing soil erosion risk in the spatial domain. The adopted approach was based on mapping procedures, such as conversion of categorical into numerical polygons, interpolation of point samples, map algebra, and raster map reclassification.

Data quality is a crucial parameter in soil erosion modeling and those errors and uncertainties are propagated to the final erosion results.

Denser grid of sampling sites for the soil survey approach would produce a better $k$ layer after interpolation although such a procedure is costly and time consuming.

## REFERENCES

1. Mammadov QS. Basics of Soil Science and Soil Geography. Vol. 229. Baku: Science; 2007.
2. Isayev AN. Influence of Groundwater on Geochemical Influence of Shirvan Plain Agro-landscapes. Baku: Works of the Azerbaijan Geographical Society; 2016. p. 41.
3. Museyibov MA. Physical Geography of Azerbaijan

Education. Bakı: SRIH; 1998. p. 81.

4. Вальков VF, Казеев KS 3rd, Колесников SI. Экологияпочв Ст.54. Ростов-на-Дону; 2004.

5. Driesen PM. Erosion hazards and conservation needs as a function of land characteristics and land qualities. In: Siderius W, editor. Land Evaluation for Land-Use Planning and Conservation in Sloping Areas. Wageningen, The Netherlands: International Livestock Research Institute; 1986. p. 32-9.

6. Valentin C, Poesen J, Li Y. Gullyerosion: Impacts,factors andcontrol. Catena 2005;63:132-53.

7. Wainwright J, Parsons AJ, Abrahams AD. Plot-scale studies of vegetation, overland flow and erosion interactions: Case studies from Arizona and New Mexico. Hydrol Proc 2000;14:2921-43.

8. Hazarika MK, Honda K. Estimates of Soil Erosion Using Remote and GİS, its Valuation and Economic Implications on Agrocultral Production, Selected Papers; 2001. p. 3-4.

9. Gregorich EG, Greer KJ, Anderson DW, Liang BC. Carbon distribution and losses: Erosion and deposition effects. Soil Tillage Res 1998;47:291-302.

10. Williams CJ, Pierson FB, Robichaud PR, Boll J. Hydrologic and erosion responses to wildfire along the rangeland xeric forest continuumin the western US: Are view and model of hydrologic vulnerability. Int J Wildland Fire 2014;23:155-72.

11. Sivakumar MV. Interactions between climate and desertification. Agric Forest Meteorol 2007;142:143-55.

12. Gitas IZ, Douros K, Minakou C, Silleos GN, Karydas CG. Multi-temporal Soil Erosion Risk Assessment in N. Chalkidiki Using a Modified USLE Raster Model. Vol. 8. EARSeL Proceedings; 2009. p. 40-52.

13. Podwojewski P, Janeau JL, Grellier S, Valentin C, Lorentz S, Chaplot V. Influence of grass soil cover on water runoff and soil detachment under rainfall simulation in asub-humid South African degrade drangeland. Earth Surf Processesand Landf 2011;36:911-22.

14. Grellier S, Kemp J, Janeau JL. The indirect impact of encroachin gtreesongullyextension: Year studyi nasubhumid grassland of South Africa. Catena 2012;98:110-9.

15. Wischmeierand WH, Smith DD. Predicting rainfall erosion losses from crop landeastof the Rocky Mountains. In: Agricultural Handbook. 28th ed. Washington, DC, USA: US Government Printoffice; 1978.

16. Williams RP. Erosion and Sediment Transportin the Owens Rivernear Bishop, California. Water-Resources Investigations Report 75-49. U.S.Geological Survey Water Resources Investigations; 1975.

17. Renard K, Foster GR, Weesies GA, Porter JP. Rusle revised universal soil loss equation. J Soil Water Conser 1991;46:30-3.

18. Bochet E, Garcıa-Fayos P. Factors controlling vegetation establishment and water erosion onmotor ways lopesin Valencia, Spain. Restor Ecol 2004;12:166-74.

19. Zuazo VH, Pleguezuelo CR. Soil-erosion and runoff prevention by plant covers review. Agron Sustain Dev 2008;28:65-86.

20. Zuazo VH, Martınez JR, Pleguezuelo CR, Raya AM, Rodrıguez BC. Soil-erosion and runoff prevention by plant cover sinamountain ousarea (SESpain): Implications for sustainable agriculture. Environmentalist 2006;26:309-19.

21. Psilovikos A, Elhag M. Forecasting of remotely sensed daily evapo transpiration data over nile Delta region, Egypt. Water Resour Manag 2013;27:4115-30.

22. Castillo VM, Martinez-Mena M, Albaladejo J. Runoff and soil loss response to vegetation removal in a semiarid environment. Soil Sci Soc Am J 1997;61:1116-21.

23. United States Department of Agriculture. Agricultural Research Service USDA-ARS. CREAMS, Afields Calemodel for Chemicals, Runoff, and Erosion from Agricultural Management Systems. Conservation Research Report 26. Washington, D.C., United States: United States Department of Agriculture; 1980.

24. Barfield BJ, Warner RC, Haan CT. Applied Hydrology and Sedimentology for Disturbed Areas. Stillwater, Okla, USA: Oklahoma Technical Press; 1983.

25. Renard GR, Foster GA, Weessies DK. McCool predicting soile rosion by water: Aguideto conservation planning with the Revised Universal Soil Loss Equation (RUSLE). In: Yoder DC, editor. Agriculture Handbook. Washington, DC, USA: US Department of Agriculture; 1997. p. 703.

26. Wilson JP, Gallant JC. Terrain Analysis Principles and Application. NewYork, NY, USA: John Wiley Sons; 2000.

27. Drzewiecki W, Wezyk P, Pierzchalski M, Szafranska B. Quantitative and qualitative assessment of soil erosion riskin Małopolska (Poland), suppor tedbyanobject-based analysis of high-resolution satellite images. Pure Appl Geophys 2014;171:867-95.

28. Mooreand ID, Burch GJ. Physical basis of the length-slope factorin the universal soil losse quation. Soil Sci Soc Am J 1986;50:1294-8.

29. Mooreand ID, Burch GJ. Modelling erosion and deposition: Topographic effects. Trans Am Soc Agric Eng 1986;29:1624-30.

30. Elhag M. Remotely sensed vegetation indices and spatial decision support system for better water consumption regime in Nile Delta. Acase study for ricecultivation suitability map. Life Sci J 2014;11:201-9.

31. Elhag M. Characterization of a typical mediterranean watershed using remote sensing techniques and GIS tools. Hydrol Curr Res 2015;6:197-204.